Crack Mitigation of Super-Long Concrete Structure

Raj Kumar BC
Graduate Student
College of Civil Engineering
Tongji University
Shanghai, China
070bce113raj@pcampus.edu.np

Zuanfeng Pan
Asso. Professor
College of Civil Engineering
Tongji University
Shanghai, China
zfpan@tongji.edu.cn

Abstract—**Due to larger dimensions of Super-long concrete structures, shrinkage and temperature effects are more pronounced and common than in typical conventional RC structures. These shrinkage and temperature effects tends to induce secondary tensile stresses which may lead to frequent cracking and excessive deflection resulting with huge losses in durability and serviceability thereby seriously affecting the safety and functionality of building structures. Nowadays, this has been the major issue that many engineers and designers are more likely to be concerned with. To date, there are many design codes and recommendations available for RC and prestressed concrete structures. However, no such codes and practices are available for the analysis, design and construction of Super-long concrete structures thus making engineers, designers and contractors completely relying on the engineering judgement based on the prior experience in similar and related projects. Hence, it requires proper clear understanding and accurate estimation of shrinkage, creep and temperature effects. This paper considers the provision of pour strip and application of prestressing (post tensioning) method as the effective means of crack mitigation in Super-long concrete structures, which is found to be both reliable and convenient according to the quantitative FEM analysis realized in ANSYS software. Furthermore, other supplementary measures in addition to prestressing is recommended to save construction costs although its effectiveness strictly depends on the actual construction site conditions.**

Keywords—super-long concrete structure, temperature, shrinkage, creep, prestressing, cracks

I. INTRODUCTION AND LITERATURE REVIEW

Sometimes referred as horizontal skyscrapers, Super-long concrete buildings are structures with larger dimensions, i.e., length, greater than 55 m (as per GB 50010-2010) [1] that requires expansion joints placed at strategic locations, which serves as a permanent measure to prevent the secondary tensile cracks that arises because of temperature variations and shrinkage of the structural concrete. However, these joints when placed at their locations, either does not maintain the structural integrity of Super-long concrete structure [2] or may cause loss of durability resulting from the leakages in case of underground parking structures [3]. In other words, the structures without joints are called as Super-long structures. Therefore, nowadays more emphasis is given to the research on structures without joints [4].

The effects of temperature changes and shrinkage are greater in ground floors or basement floors of the building structure [5] and hence they are given more importance for crack control provisions of basement floor slab. Also, the effect of temperature cannot be ignored when the structure is superlong [6].

The combined effects of shrinkage, creep and temperature drop tend to induce the tensile stresses in the basement slab, with shrinkage and temperature effects often being more pronounced than creep, since creep induced stresses in concrete are often relaxed with time due to relaxation in concrete [7]. The combined shrinkage and temperature effects also decreases due to relaxation coefficient when creep effects are considered in the analysis [8].

Till date, many crack mitigating methods like use of shrinkage compensating concrete (SCC), prestressing, pour strip and sequential construction, addition of extra steel reinforcements, etc. have been adopted for eliminating the shrinkage and temperature cracks in Super-long concrete structures. Various researchers have conducted research on crack control of super-long concrete structures employing different methods.

Gerard [9] studied the design and construction technology of expansion reinforcing band and use of shrinkage compensating concrete in super-long concrete structure in elastic foundation considering Soil Structure Interaction and then compared with

conventional concrete structure. In engineering practice, this method has been used to control cracking and leakage problems, this practice ultimately eliminates the expansion joints in the super-long concrete structure as well.

Also, the concept of prestressing to eliminate secondary tensile stress is not new. As many researchers have carried out the study regarding the prestressing application in crack controlling of super-long concrete structures [2], [10]–[13] and is found to be most effective and convenient means for reducing tensile stresses in structural concrete.

This study focuses on mitigation of the cracks that are induced by the shrinkage, creep, and temperature variations. This can be achieved by the application of post tensioning in the basement slab of Super-long building and setting of a post-poured strip along the transverse direction, including the elastic foundation (i.e., springs) for soil structure interaction (SSI) that provides restraints due to the connected pile foundations underneath. Here, post-poured strip is employed as a temporary measure for reducing the amount of anticipated shortening that takes place before its closure, which is basically characterized by the plot of shrinkage plus creep shortening versus time. Hence, the effectiveness of the post poured strip strictly depends on its open time. Also, the sequential construction method becomes convenient with the setting of pour strip.

The location of the pour strips (or expansion joints) varies accordingly as the ambient temperature of the site and can be estimated using deformation distribution method. More detailed description about evaluating the position of pour strips is given in the literature [14]. However, the pour strip in symmetrical basement plan structure is usually placed at the middle to ensure even distribution of stresses.

In this paper, the study is the combined application of research conducted by Li and Sha [10] for prestressing and setting of post-poured strip, and Gerard [9] for elastic foundation.

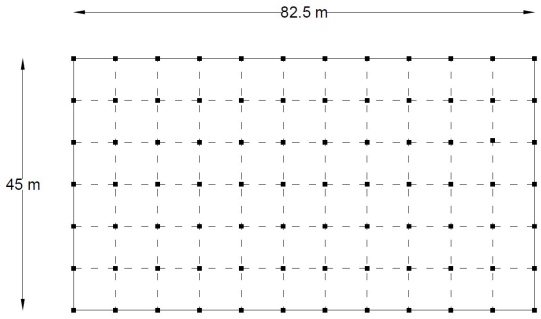

Fig. 1. Basement floor plan of the Super-long building

II. PARAMETERS CONSIDERED

The required parameters for the analysis are considered according to the real engineering field conditions. While some of the parameters are assumed such that it applies for typical Super-long structures.

For the analysis, a fictitious Super-long concrete multi story building to be constructed in Shenzhen, China is assumed with overall plan dimensions of 82.5 m × 45 m (Fig. 1), in which longitudinal direction consists of 11 spans each of length 7.5 m and transverse direction consists of altogether 6 spans each of length 7.5 m. The thickness of the basement slab being 500 mm. The compressive strength for basement slab concrete is 35 MPa and the average precompression level of 1.5 MPa is applied to transfer the effective prestress after all prestress losses. Also, the building is assumed to be constructed at site where average annual ambient relative humidity is 70 % and seasonal temperature variations is 15 ℃. For early application of post tensioning at about 5 days, it is noteworthy to ensure that concrete gains adequate strength to sustain applied prestressing force. Thus, the casted basement concrete slab is cured for first 3 days to gain adequate strength and then, allowed to shrink. It is also assumed that the concrete mix is designed to reach its ultimate creep and shrinkage at about 75 years. This indicates shrinkage and creep predictions and their effects also applies to other long concrete structures of similar life span. The stress and deformation analysis are carried out for only the basement slab whereas the analysis of upper floors is not under the scope of this study.

For stress distribution analysis of the basement slab, first the accurate prediction of shrinkage and creep is necessary. The prediction of shrinkage and creep depends upon the concrete paste parameters, strength parameters, loading parameters and environmental conditions. In other words, quantification accuracy of these parameters is based on real engineering site conditions (non- standard conditions). Then, the stress induced due to shrinkage, creep and temperature effects are predicted and examined for possibility of cracking and to suggest other crack mitigation measures. Hence, the suitable prediction model for shrinkage and creep is selected on the basis of its ease in application and simplicity in calculations.

III. SHRINKAGE AND CREEP PREDICTIONS

A. Comparison between different shrinkage and creep prediction models

The most popular and latest models for prediction of creep and shrinkage are ACI 209R-92, CEB-FIP 2010, GL 2000 and B3. With reference to the various literatures [15]–[17], these four prediction models are compared according to their accuracy, ease in application, total no. of parameters used, etc. As for code models, the ACI 209R-92 model requires the

greatest number of parameters while CEB-FIP 2010 and GL 2000 models require the least. Apart from code models, B3 model required the most parameters since it was developed based on the ACI 209R-92 model. The GL 2000 model required less parameters since it was developed based on both ACI 209R-92 Model and CEB-90 model. In GL 2000 model, creep and shrinkage predictions can be done with a simple procedure as all the equations have been formulated in terms of strength development of concrete with time. Hence, GL 2000 model is utilized to predict shrinkage and creep.

B. GL 2000 Model

The current version of GL 2000 model [16] was introduced by Gardner in 2004 with slight modifications of some coefficients from its older version (Gardener and Lockman, 2001) [18]. This model employs a simple procedure for creep and shrinkage prediction that requires less parameters even for a more complicated model. And the creep and shrinkage predictions can be easily improved by evaluating concrete strength development with time and modulus of elasticity (ACI 209, 2008) [19].

To ensure the deviations of both shrinkage and creep predictions to be within ±25%, GL 2000 model has following parameter restrictions.

- Mean compressive strength of concrete from 16 - 82 MPa
- *w/c* ratio ranges from 0.4 - 0.6
- Concrete *v/s* ratio greater than 19 mm
- The age of concrete at loading and the age of concrete at the start of drying should be at least 1 day ($t_o \geqslant t_c \geqslant 1$ day)
- For type I, II and III Portland cements
- Relative humidity ranging between 20–100 %

The following parameters are required for prediction of shrinkage and creep using GL 2000 model

- Age at which drying starts (or age at the end of moist curing)
- Age at loading
- Relative Humidity (in decimal)
- Volume-surface ratio
- Cement type
- Mean compressive strength of concrete at 28 days

C. Prediction equations of shrinkage and creep using GL 2000 Model

Shrinkage

The shrinkage, $\varepsilon_{sh}(t, t_c)$ at any age, t by GL 2000 model is predicted as

$$\varepsilon_{sh}(t, t_c) = \varepsilon_{shu}\, \beta(h)\beta(t - t_c) \quad (1)$$

$$\varepsilon_{shu} = 900k \left(\frac{30}{f_{cm28}}\right)^{0.5} \times 10^{-6} \quad (2)$$

$$\beta(h) = (1 - 1.18h^4) \quad (3)$$

$$\beta(t - t_c) = \left[\frac{(t - t_c)}{(t - t_c) + 0.12\left(\frac{V}{S}\right)^2}\right]^{0.5} \quad (4)$$

where,

ε_{shu} is the ultimate shrinkage strain

$\beta(h)$ is the correction factor for the effect of RH

$\beta(t - t_c)$ is the correction factor for the effect of time of drying

$f_{cm28} = 1.1f_c^{'} + 5$, is the mean compressive strength of concrete

$f_c^{'}$ is the characteristics compressive strength

$k = 1.0$, depends on the cement type

h is the relative humidity in decimal

$\frac{V}{S}$ is the volume-surface ratio in mm

t_c is the age at which drying starts

Creep

Creep is predicted in terms of creep compliance, $J(t, t_o)$ and then it is converted into creep strains by multiplying with the applied precompression (1.5 MPa) and stress reduction factor (0.5).

$$J(t, t_o) = \frac{1}{E_{cmto}} + \frac{\phi_{28}(t, t_o)}{E_{cm28}} \quad (5)$$

$$\phi_{28}(t, t_o) = \phi(t_c)\left[2\frac{(t-t_o)^{0.3}}{(t-t_o)^{0.3}+14} + \left(\frac{7}{t_o}\right)^{0.5}\left(\frac{(t-t_o)}{(t-t_o)+7}\right)^{0.5} + 2.5(1 - 1.086\, h^2)\left(\frac{(t-t_o)}{(t-t_o)+0.12\left(\frac{V}{S}\right)^2}\right)^{0.5}\right] \quad (6)$$

$$if\ t_o = t_c,\ \phi(t_c) = 1$$

$$if\ t_o > t_c,\ \phi(t_c) = \left[1 - \left(\frac{t_o - t_c}{(t_o - t_c) + 0.12\left(\frac{V}{S}\right)^2}\right)^{0.5}\right]^{0.5} \quad (7)$$

where,

E_{cmto} is the Elastic modulus at the time of loading

E_{cm28} is the Elastic modulus at 28 days

$\phi_{28}(t, t_o)$ is the creep coefficient, the ratio of creep strain to elastic strain

$\phi(t_c)$ is the correction factor for the effect of drying before loading

TABLE I. 'S' AND 'K' VALUES AS A FUNCTION OF CEMENT TYPE

Cement type	S	k
Type I	0.335	1.0
Type II	0.4	0.75
Type III	0.13	1.15

Ultimate creep and shrinkage	micro strains
Creep	117.6
Shrinkage	474.6
Total	592.2

TABLE II. ULTIMATE STRAINS

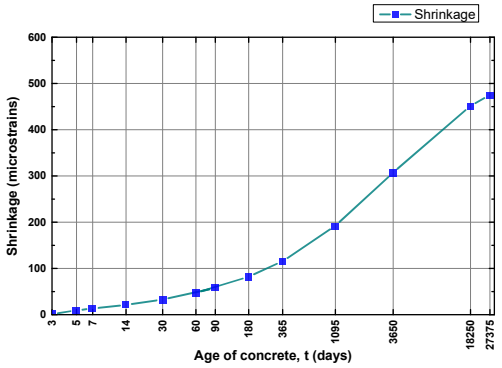

Fig. 2. Shrinkage predictions

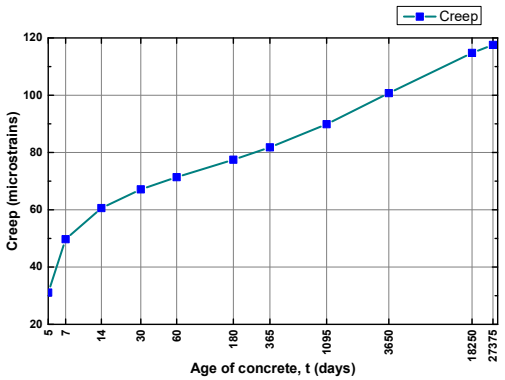

Fig. 3. Creep predictions

Also, Modulus of elasticity has been defined as:

$$E_{cmt} = 3500 + 4300\sqrt{f_{cmt}} \quad (8)$$

And Time dependent strength is given by:

$$f_{cmt} = \beta_e^2 f_{cm28} \quad (9)$$

$$\beta_e = \exp\left[\frac{s}{2}\left(1 - \sqrt{\frac{28}{t}}\right)\right] \quad (10)$$

s being the CEB style strength development parameter which depends on the cement type (TABLE I.).

D. Shrinkage and creep prediction results

The shrinkage and creep predictions expressed in microstrains are shown in Fig. 2 and Fig. 3.

E. Ultimate shrinkage and creep

The predicted ultimate shrinkage and creep strain as obtained from Fig. 2 and Fig. 3 is depicted in TABLE II.

F. Restraint to shortening effects

Since, the post tensioning is to be applied in the Super-long basement slab, the Super-long structure is treated as long PT slab with enough restraints provided by the foundations. The PT concrete floor design handbook[20] recommend considering the restraint to shortening (RTS) effects based on any one of the following criteria.

- the prestress to exceed 2 MPa
- the floor slab structure has larger dimensions

The overall dimensions (45 m × 82.5 m) of the overlong basement slab and presence of stiff columns that restraint the shortening of the floor makes RTS effects more significant. The analysis of the effects of shortening is done by detailed calculation of elastic, creep, temperature and shrinkage shortening and then compute the force required to deflect the supports by estimated amount of shortening at points of support. However, this restraint force calculation [21] is not under the scope of this study.

G. Shortening

Like typical PT construction, Super-long concrete basement floor shortening due to elastic compression, concrete creep, shrinkage can be expressed as approximately 25 mm (1 in.) per 30.5 m (100 ft) [22]. However, this total shortening values differ according to the quantifying parameters involved in evaluation and construction site conditions. Here, the detailed calculation of shortening including temperature for 30.5 m (100 ft) PT slab is done by multiplying the predicted strain with length of the floor slab as in TABLE III. below.

TABLE III. SHORTENING IN MM PER 30.5 M (100 FT) SLAB

Type	Shortening	
	(mm)	(%)
Temperature shortening	4.58	19.4
Elastic shortening	0.95	4
Creep shortening	3.59	15.2
Shrinkage shortening	14.48	61.4
Total shortening	23.59	

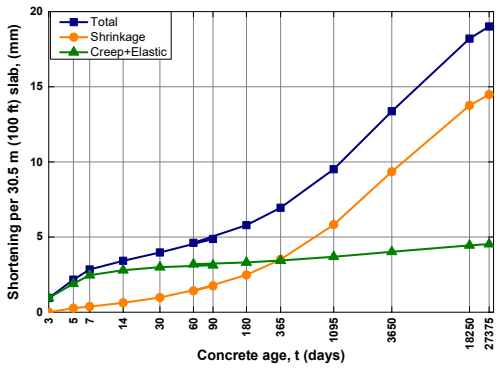

Fig. 4. Shortening values in mm per 30.5 m slab (100 ft) without temperature shortening

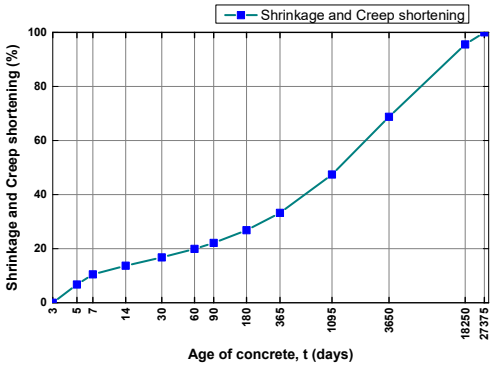

Fig. 5. Shrinkage and creep shortening, %

The elastic and creep shortening, caused by the prestressing force are often compared in terms of their shortening ratio. The result based on TABLE III. shows that shortening due to concrete creep is 3.8 times of elastic shortening for GL 2000 model. Whereas, PT concrete floor design handbook recommended [20] the ratio of 2.5, without taking into account of stress reduction factor for elastic shortening. On the contrary, this stress reduction factor (0.5) included in present study reduces the elastic and creep shortening to half for sequential stretching in unbonded post tensioning.

TABLE III. also shows that the shrinkage is the largest contributor i.e., about more than 60% and temperature being the second most about 20% of overall shortening. Meanwhile, creep shortening accounts for 15% and elastic shortening contributes for about 4% for shrinkage and creep prediction using GL 2000 model.

Fig. 4 indicates how the shrinkage shortening, creep plus elastic and total shortening vary with time, without considering the temperature.

Fig. 5 shows the percent of final shrinkage and creep shortening which is utilized for determining the short-term shortening of slab. The current study involves the incorporating of post poured strips in design, which remains open for the specific period such that an anticipated amount of shortening has taken place until its closure. Besides reducing the shrinkage, provision of pour strip also helps in complete elimination of the elastic shortening.

H. Pour strip open time

The pour strips opening time is quite important as it identifies the amount of shortening occurred before and after the closure of pour strips. The placement of pour strips at midway is due to architectural requirements and the construction requirements i.e., ease in placement and stressing of tendons. The pour strips open time can be estimated as mentioned in Fig. 5, especially taken at least 30 days, but more precisely depends upon the % of shortening that has taken place within that specified period. Fig. 5 shows the 30 days, 60 days, and 90 days percentage is estimated to be approximately 17%, 20% and 22% of total shortening respectively. The appropriate pour strip opening time is chosen somewhere in between 30-90 days such that maximum percentage of shortening occurs within that stipulated time and on the other hand, construction of the structure is not delayed. Here, 90 days concrete age possess enough anticipated shortening and open time greater than that will delay the construction schedule. Thus, 90 days open period will benefits the construction project taking into consideration of both criteria, hence optimizing the project completion time frame.

To elaborate and better understand the effect of post poured strip in Super-long PT slab, the section of the basement slab with columns along the central grid from the basement slab plan in Fig. 1 is considered. The estimated amount of floor shortening at support points is important to understand the RTS effects and beneficial use of pour strip.

The PT slab tends to shorten in the direction towards the stationary point. Here, the stationary point refers to the center of stiffness or the center of mass for symmetrical structure [23]. Thus, it is obvious that the shortening of slab calculated at far end point is greater than shortening at any near points. The shortening at the column points is calculated by multiplying the total strain in concrete by the distance of specified columns from stationary point. The representation of reduction of shrinkage shortening at columns locations when using pour strips are shown in TABLE IV. and TABLE V. The shortenings are computed at columns locations up to the midway of the slab for symmetric section.

TABLE IV. SHRINKAGE SHORTENING AT COLUMN LOCATIONS (W/O POUR STRIP)

	Column	column location from center of stiffness (C.O.S) (m)	total shortening (mm)
Without pour strip	C1	41.25	19.6
	C2	33.75	16.0
	C3	26.25	12.5
	C4	18.75	8.9
	C5	11.25	5.3
	C6	3.75	1.8

TABLE V. SHRINKAGE SHORTENING AT COLUMN LOCATIONS (WITH POUR STRIP)

	Column	before 90 days		after 90 days		total shortening (mm)	percent reduction
		Column location from C. O. S (m)	Shortening (mm)	Column location from C. O. S (m)	Shortening (mm)		
With pour strip opened for 90 days	C1	18.75	1.1	41.25	17.2	18.3	6.6
	C2	11.25	0.6	33.75	14.1	14.7	8.1
	C3	3.75	0.2	26.25	11.0	11.2	10.4
	C4	3.75	0.2	18.75	7.8	8.0	9.7
	C5	11.25	0.6	11.25	4.7	5.3	0.0
	C6	18.75	1.1	3.75	1.6	2.6	N/A

Note: N/A means not available (or expansion occurs instead of shortening)

The shortening at columns locations at the slab ends due to shrinkage only are reduced by more than 6 %. Here, this reduction nature of shrinkage shortening is similar to creep shortening since the shrinkage and creep are time dependent and perfectly cope with the construction sequence. While, elastic and temperature shortening behavior at columns locations are different because elastic shortening occurs at the time of prestressing and temperature shortening occurs throughout the life of the structure.

IV. SOIL STRUCTURE INTERACTION EFFECT

The concrete stress is directly affected by the type of the foundation connections being considered. Stress changes at center spans of the basement slab is based on the theory of fixed, pinned, or partially fixed connections to the pile foundations. There is more reduction of concrete stress in slab when using fixed connection, while the concrete stress reduction for partially fixed connections lies somewhere in between the fixed and the pinned connections [7]. The fixed connections strictly overestimate the volume change restraint forces whereas pinned connections underestimate it. These connections are based on partial fixity values in which the interaction between the soil and the structure is disregarded [21].

Moreover, the PCI Design Handbook[21] recommends a method to compute the rotational stiffness of the foundation supports based on the allowable soil bearing stress value, but it is quite limited to isolated footings. In contrast, the present study considers the effects of pile foundation as the foundation restraints, thus PCI method is disregarded. In other words, the foundations consideration can be done regarding the soil-structure interaction (SSI) [7], which is the main basis of geotechnical perspective, although the study is not done in overall depth, in this study.

It is of utmost importance to accurately predict the effects of overall shortening in basement structures against restraints from the foundations. Fig. 6 shows how the column supports and their interaction with soil is replaced by the series of elastic springs and referred as SSI. This SSI effect is more precisely explained by Winkler's model. Winkler´s Model [24] has been best recognized by subgrade reaction of the soil represented as an elastic medium, by replacing the soil by a set of infinitely, closely spaced, and independent elastic springs. The lateral stiffness of the springs k_h, is evaluated based on the *p-y* method. Where, *p* being the stiffness ratio between the soil reaction in one meter length of pile and *y* being the deflection.

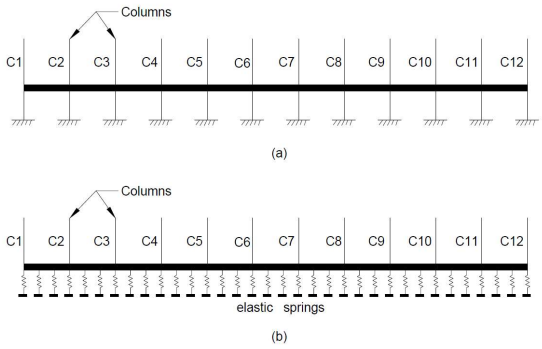

Fig. 6. Full basement slab sections from fig 1, (a) w/o SSI, (b) with SSI

All springs connected in the slab are assumed to behave linearly-elastic until failure stage is reached, at this stage the force remains constant while the spring may undergo additional deformation [25]. According to various literatures, k_x is calculated depending on the type of foundation and its properties, elastic modulus, plasticity and creep, exhibiting strictly non-linear behavior and making it difficult for evaluation. Wang [26] has proposed empirical values of k_x for different types of soil by conducting the various experiments. Due to less available soil parameters, assuming the soft soil at the project site situated in Shenzhen, China, the horizontal stiffness k_x of 1×10^4 KN/m^3 is taken for soil thickness of 5 m.

V. FEM ANALYSIS

ANSYS [27] is a finite element analysis software used for engineering simulation which integrates different types of analysis fields. Due to its powerful modeling capability for finite element analysis of large structures, ANSYS has been widely used in civil engineering application. In this study, the structural deformation and stress analysis is done considering a linear elastic model. For the super-long concrete structure, the stress and strain distribution analysis of the basement slab is examined under the effects of equivalent temperature deformation. Thus, SHELL63 and COMBIN14 elements shown in Fig. 7 are used to simulate the concrete floor and foundation restraints respectively in finite element modeling.

SHELL63 element has both bending and membrane capabilities. Also, both in-plane and out of plane loads can be applied. The element has six DOF at each node i.e., translations and rotations in all three axes. Stress stiffening and large deflection capabilities are also included. On the other hand, **Combin14** element has 1-D, 2-D or 3-D applications in axial or twisting behavior. The axial spring-damper is a 1-D either in tension or in compression. Each of its nodes consists of 3 DOF (all axial) along all three axes.

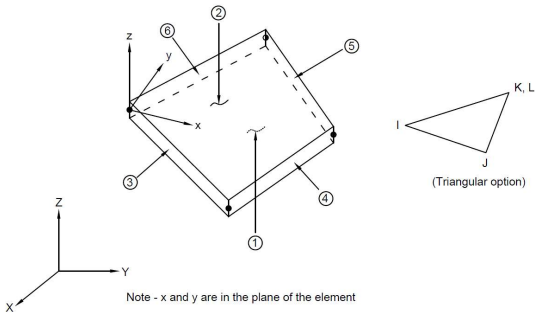

(a)

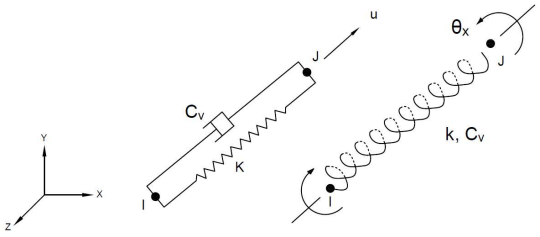

(b)

Fig. 7. Element geometry, node locations and the coordinate system of (a) SHELL 63, and (b) Combin 14 [27]

A. Restraints due to pile foundation

In modeling, the representation of **the restraints due to pile foundation** on the floor slab is modelled by considering the spring stiffness in three directions. Hence, the foundation stiffness, K_x is the input value of x-direction stiffness for spring element which represents the out of plane stiffness, and its matrix is augmented by 3 or 4 springs to ground. The no. of springs equals no. of distinct nodes, and their direction being normal to the plane of the element [27]. The resultant stiffness is adjusted according to influence area and no. of distinct nodes, which depends on mesh element edge length (2500 mm) as follows:

$$K_{x,i} = a.A.\frac{K_x}{N} \tag{11}$$

Where, $K_{x,i}$= out of plane stiffness at node i, $a.A$= influence area, N = no. of distinct nodes, K_x= spring stiffness (input as EFS on R command in ANSYS apdl), a is the influence area multiplier whose value depends upon the locations of springs and provided as 1, 0.5 and 0.25 for springs at interior, edge and corner respectively.

Ansys automatically computes the three stiffness values for each different direction for springs based on their locations, provided that the value of K_x is used as an input. Here, K_x= 1×10^4 KN/m^3 is taken according to section IV.

Whereas, the y-direction stiffness is same as that of x-direction stiffness and z-direction stiffness can be adjusted as:

$$K_z = 1.43 \times K_x \tag{12}$$

B. Assumptions

The following assumptions are made in the finite element analysis.

- The equivalent temperature as prestress is applied in terms of axial load in x-direction in concrete slab.
- The effective tendon stresses that changes with time and tendon geometry profile are not

considered in the analysis. Moreover, tendon behavior has negligible effect on the stress distribution profile.

- Combination of shrinkage and temperature drop is assumed as an equivalent temperature drop.
- Only x-direction axial stresses are examined for all body temperature loads applied.
- Building during construction is exposed to external environment, it means the temperature drop when combined with concrete shrinkage makes the situation more serious.

C. Prestressing simulation

Post tensioning is simulated in the form of precompression in the Shell63 element using equivalent prestress temperature load, because the Shell63 element in ANSYS apdl does not allow the direct application of prestress. Thus, the application of temperature rise as body temperature load plays the key role in inducing the adequate precompression in the slab model. There is no doubt that prestress temperature rise reduces the induced stresses, however, the level of stresses eliminated through prestressing can be main approach of this analysis. Also, there is no direct prestress transfer from the unbonded tendons to the concrete through the bond although prestressing is done and transfer occurs through the slab end in real practice. This equivalent prestress load in FEM analysis is valid only in case of unbonded post-tensioned concrete members since it is not possible to justify the tendons profile and geometry in Shell 63 element for bonded prestressed members. The following relation depicts the prestress temperature.

Prestress strain, $\varepsilon_p = \frac{f_{cpa}}{E_{cmto}} = \frac{1.5}{26058.41}$

And equivalent temperature, $T_p = \frac{\varepsilon_p}{\alpha} = 5.76\ ℃$

where,

f_{cpa} is the average precompression in concrete

E_{cmto} is the elastic modulus of concrete at the time of stressing

α is the thermal expansion of normal concrete often taken as 1×10^{-5} / ℃.

D. Simulating shrinkage and creep shortening

The shrinkage or creep shortening effects and temperature drop effects in a concrete slab are quite similar according to the study of Mohammad [28]. Also, the combined effects of shrinkage and temperature drop is critical for a Super-long concrete structure and hence the detail FEM analysis is conducted especially incorporating concrete shrinkage and temperature drop due to external temperature variations. However, creep shortening effect is due to prestressing and is often relaxed at later ages due to concrete relaxation, and is not considered in detail FEM analysis, except in the case of age adjusted effective modulus.

E. Age adjusted elastic modulus

First developed by Trost, Age adjusted effective modulus (AAEM) can be easily applied in various concrete structures since it has better theoretical accuracy than other methods incorporated in creep analysis [19]. Furthermore, the non-linear behavior of the concrete structures can be predicted accurately by using AAEM in linear elastic analysis. The age-adjusted effective modulus is estimated as

$$E_{ct} = \frac{E_c(t_o)}{1+\varphi(t,t_o)\times\chi(t,t_o)} \qquad (13)$$

Where, $\chi(t,t_o)$ is the aging coefficient which is determined from the evaluation of the stress relaxation function. The aging coefficient depends on the loading age, ultimate creep coefficient and the time gap after the loading is applied and $\varphi(t,t_o)$ is the creep coefficient.

F. Temperature variations

1) Temperature gradient

Temperature variations may be taken as daily, seasonal, or yearly temperature difference values. This study uses seasonal temperature drop as temperature gradient whose value is taken as -15 ℃. This value is assumed to be constant for the analysis of basement slab throughout the construction and service period. But its effects are examined only for the early construction period as the effects of temperature drop is quite significant during construction unless the thermal insulation measures are applied. Its effect is taken negligible after the construction, provided that the building is installed with thermal insulation measures or proper heating systems[14].

TABLE VI. ELASTIC MODULUS AND TEMPERATURE SHRINKAGE WITHOUT POUR STRIP

Model	Type	E[a] (N/mm^2)	Temperature[b] (T_{sh})
1	Conventional concrete slab	6944.6	-47.46 ℃
2	Post tensioned concrete slab	6944.6	-47.46 ℃

[a] E represents age adjusted effective modulus (AAEM)

[b] T_{sh} represents only ultimate shrinkage temperature and negative sign means contraction

TABLE VII. ELASTIC MODULUS AND TEMPERATURE SHRINKAGE BEFORE AND AFTER CASTING OF A POUR STRIP

Model	Type	Before 90 days		After 90 days	
		E(N/mm^2)	Temperature (T_{sh1})	E (N/mm^2)	Temperature (T_{sh2})
3	Conventional slab	10969.2	-5.736	6944.6	-41.724
4	Post tensioned slab	10969.2	-5.736	6944.6	-41.724

2) Shrinkage Temperature (before 3 months)

The equivalent shrinkage temperature, T_{sh1} at 90 days is obtained from shrinkage before setting of the pour strip is given as

$$T_{sh1} = \frac{\varepsilon_{sh}(90)}{\alpha} = \frac{57.36\times10^{-6}}{10^{-5}} = -5.736\ ℃$$

3) Shrinkage Temperature (after 3 months)

The relative equivalent shrinkage temperature difference, T_{sh2} obtained as a result of shrinkage that occurs after the closure of post strips and is stated as

$$T_{sh2} = \frac{\varepsilon_{ult}-\varepsilon_{sh}(90)}{\alpha} = -41.724\ ℃$$

Where, $\varepsilon_{sh}(90)$ is the shrinkage strain predictions at first 90 days. And, ε_{ult} is the ultimate shrinkage strain for GL 2000 model.

The shrinkage temperature T_{sh} in TABLE VI. denotes the temperature corresponding to ultimate shrinkage. Whereas, the shrinkage temperatures T_{sh1} and T_{sh2} in TABLE VII. for models 3 and 4 respectively are taken differently to manipulate the construction sequence of the structure. And, E is the AAEM, the representation factor of creep effects, when taken into account for elastic analysis.

G. Superposition - main focus of the study

Li and Sha[10], studied the application of prestress technology in Super-long concrete structures, considering the shrinkage and temperature effects but the combined temperature stress of each slab before the closure of post poured strip is not considered. In contrast, the combined stress analysis in present study is based on the method of superposition of stress as studied by Gerard [9] because it allows the engineers and designers to analyze the resultant stress behavior of the Super-long structure starting from early construction period up to its whole service life.

H. Comparative analysis

Based on the above parameters, following four models are taken for the analysis to examine the stress distribution in x-direction of the Super-long post tensioned basement slab as well as the effect of the post-poured strip. The study also examines the stress distribution in Super-long conventional RC slab, for both with and without pour strips cases, making a basis of its comparison with corresponding post tensioned concrete slab.

- **Model 1 (Conventional concrete slab):** The basement slab as a whole is casted at a time, finite element analysis is conducted including equivalent combined temperature load at ultimate, without post poured strips and post tensioning operation.
- **Model 2 (Post-tensioned concrete slab):** Alike model 1, model 2 is quite similar in all construction aspects, except the model 2 exhibits application of prestress load at 5 days.
- **Model 3 (Conventional concrete and pour strip open time - 90 days):** The outer concrete slab (pour 1 in Fig. 8) is initially casted while a post-poured strip (pour 2 in Fig. 8) of width 2 m is casted at 90 days. The total stresses developed will be the superposition of stresses induced due to the temperature load equivalent up to 90 days for the outer slabs, and the full structure at ultimate after the closure of the post-poured strip.
- **Model 4 (Post tensioned concrete and pour strip open time – 90 days):** Model 4 represents the model 3 with prestress applied in the form of initial equivalent temperature load at 5 days. The total stresses developed as the result of superposing stresses due to the temperature load equivalent to 3 months for the outer slabs, and the structure as a whole at ultimate after the closure of the post-poured strip are analyzed and examined.

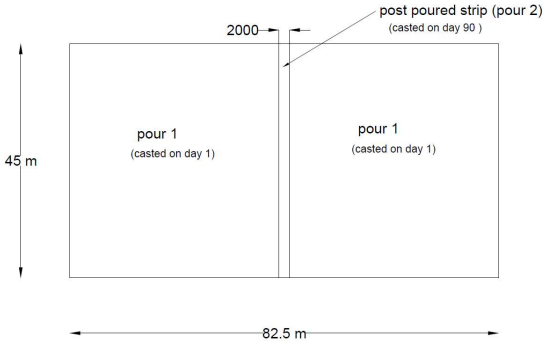

Fig. 8. Basement plan representing the construction sequence

VI. RESULTS AND DISCUSSIONS

A. Finite Element Modeling Results

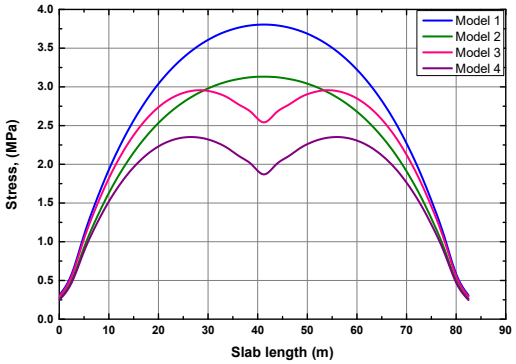

Fig. 9. Stress distribution in a Super-long concrete basement slab

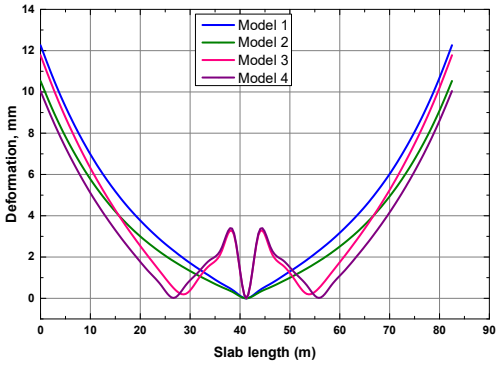

Fig. 10. Deformation distribution in a Super-long concrete basement slab

B. Stress analysis results

The superposition method is applied for different temperature loads due to shrinkage, external temperature and prestress. The plot of stress distribution after superposition along longitudinal x-direction against the slab length is shown in the Fig. 9. The parameters for the four different analysis model are shown in TABLE VI. and TABLE VII.

Fig. 9 indicates the stress difference between model 1 and model 2 caused by the application of prestressing follows parabolic distribution, it differentiates the Super-long conventional slab from Super-long post tensioned slab, without pour strip. The maximum induced stress appears at center spans of the slabs while minimum stress at end spans. The difference is also maximum at center and least at ends. The presence of equal mesh element size and restraints with same stiffness values maintains the integrity and symmetry of the Super-long slab structure, hence the stress distribution profile becomes symmetric. The maximum stress examined in the conventional and post tensioned slab are 3.8 MPa and 3.15 MPa respectively with maximum stress difference of about 0.65 MPa.

Stress distribution between model 3 and model 4 caused by the application of pour strip implies that Fig. 9 differentiates the Super-long conventional slab from Super-long post tensioned slab, with pour strip. Since, presence of pour strip disintegrates the Super-long slab structure into two different slabs (pour 1) that have similar behavior i.e., with respect to temperature and shrinkage effects, the slab tends to shorten towards the center of stiffness or point of zero movement. The maximum induced stress appears at near the center of the individual slabs while minimum stress is induced at the ends. Also, the difference is maximum at the center of the individual slabs and least at the ends. The maximum stress examined in the conventional and post tensioned slabs are 3 MPa and 2.3 MPa respectively on either side of the pour strip with stress difference of about 0.7 MPa.

From model 1 to model 4, stress reduces from 3.8 MPa to 2.35 MPa. Here, the induced stress difference is maximum as model 4 is obtained after the combined effect of pour strip and prestress, Thus, taking it as the final model for further prestress design.

C. Deformation analysis results

Fig. 10 shows the deformation distribution after superposition along length of the Super-long concrete structure. The length verses deformation curve is symmetric and follows parabolic distribution with maximum values at both ends and minimum at the center for all models. This maximum deformation at ends may affect the corresponding column capacities. Due to this reason, it is appropriate to consider the effects of temperature and shrinkage on capacity of columns with maximum deflection. In addition, for model 3 and model 4, abrupt change in deformation is observed around the location of post poured strip.

TABLE VIII. COMPARISON OF END DEFORMATIONS

Slab end deformations (mm)	
Theoretical value (shortening)	**FEA Model value (deformation)**
18.3	11.9

D. The effects of restraints

Due to the pile foundation restraints, average precompression values of the basement slab is found to be maximum at the edge of the slab and gradually decreases further towards the center, showing parabolic distribution. However, the stress distribution and stress path along x-direction shows the similar characteristics with FEA model results presented by Guo et, al, [3] Moreover, similar structural behavior when compared with the model results obtained by Guo et, al, maintains validity to the model.

The calculated end shrinkage shortening, and end shrinkage deformations obtained from FEM analysis are compared to address the effects of restraints is shown in TABLE VIII. And it is obvious that the restraints decrease the deformations to some extent. Thus, there exists a certain coefficient that directly decreases the deformation of the super-long slab and specifically represented by constraint coefficient or degree of restraint. Here, the constraint coefficient is the equivalent constraint of all the stiffness associated with the elastic springs and its relationship with the shrinkage strain is represented as

$$\varepsilon_R(t) = \varepsilon_{sh}(t) \times \eta \qquad (14)$$

Where, $\varepsilon_R(t)$ is the restrained shrinkage strain, $\varepsilon_{sh}(t)$ is an unrestrained or free shrinkage strain and η is the constraint coefficient. Since, end deformation increases or decreases accordingly as shrinkage strain. $\eta = 0.65$ is computed as the ratio of shortening and deformation from TABLE VIII. This computed coefficient is quite within the limit range 0.6 - 0.8, as mentioned in the various literatures for Super-long RC structures.

The presence of the restraints directly decreases the precompression level in the basement slab. However, this reduction in the precompression in slab has no influence in the strength and capacity of the structural member [7]. And the prestress losses also remain unaffected by the reduction in the precompression level that results from the foundation restraints. Hence, in order to make this prestress effect more effective in the basement floor, the sequential construction method is adopted [3] such that prestress applied is effectively transferred to concrete, without any huge precompression losses, before introducing the stiff structural elements (basement perimeter walls) in the basement.

Thus, obtained maximum stresses and deformations might cause cracking in the slab at sections where stress exceeds the tensile strength of the resisting concrete. Hence, the proper engineering judgement is also required for analysis of the above results and apply suitable prestress level for mitigating the cracks that may be caused by the superposed stresses.

E. Prestress Design

The prestressing is done after the concrete slab attains adequate strength. Here, strength denotes the compressive as well as tensile strength. Compressive strength for resisting enough of the initial jacking force and tensile strength to assure that the cracks are not formed after prestress transfer. Both of these strengths increase with time. The precompression added up with the tensile strength for reducing or eliminating the secondary tensile stresses caused as a result of shrinkage, creep and temperature. Maximum net tensile stress after effective prestress transfer and pour strip effect that is responsible of crack formation in Super-long basement slab is from model 4 i.e., 2.35 MPa. For no crack formation within the basement slab, tensile strength of concrete at ultimate stage should exceed 2.35 MPa. Using ACI 209 code [19], tensile strength of the concrete yields 2.412 MPa, which illustrates that prestressing has been quite effective in cracks mitigation of Super-long concrete structure.

Therefore, use of unbonded post tensioning is found as an effective method, also applications of unbonded tendons have some additional advantages with important features like flexible tendon layout, easy tensioning and anchorage, and high strength. The prestress design is done according to the requirements due to the net induced stresses obtained from stress distribution results. The maximum tensile stress is at the middle section of the basement slab denotes that the greater prestress level shall be required or the c/c distance between the unbonded prestressing strand at central part of the structure should be reduced, while a medium prestress level is sufficient at the ends. The unbonded tendons with low relaxation strands of grade 1860 MPa, 12.7 mm diameter @400 mm c/c spacing at ends and @ 300 mm c/c spacing at center may be an effective solution against the cracking.

F. Other Additional crack mitigation measures

Applicable only if the secondary tensile stresses are still in excess of tensile strength of the concrete and often applied as a supplementary measure in addition with prestressing.

- Resistance and release.

- Shrinkage compensating concrete (SCC): SCC induce prestress by increasing the volume of the concrete at initial ages or decreasing the stress caused by shrinkage and temperature [29]. Shrinkage compensating concrete also helps post tensioning operation by reducing the costs that is required for installing the certain sophisticated details like slip joints, wrapped dowels and additional steel reinforcement, etc.
- Use of anti-cracking fiber reinforcing.
- Non prestressed reinforcement addition.
- Reducing the temperature gradient during construction can also be the promising measure to decrease the temperature shrinkage.

VII. CONCLUSIONS

This paper utilizes the theoretical evaluation of the shrinkage, creep and temperature effects, benefits of post-poured strip and post tensioning, and finite element analysis of the Super-long basement slab using linear elastic model. The key conclusions drawn from the analysis are:

- Shrinkage contributes the most in total shortening of the Super-long structures, temperature being second-most while creep and elastic shortening effects due to prestressing are less as compared to that of shrinkage and temperature effects due to relaxation that occurs with time.
- The end deformations of the Super-long basement slab are greater than center spans deformation. This indicates that columns at the ends are more likely to undergo greater deflection and hence columns capacity should be considered in the analysis and design of Super-long structures.
- The combined tensile stress is found to be greater at the center spans than at end spans, due to which the center spans of the basement floor is to be equipped with more tendons (less c/c spacing between tendons) or higher prestress level can be applied at vulnerable sections.
- Relaxation of the structural concrete used in the form of relaxation function is associated with the AAEM in this study and must be considered for detailed study because apart from creep and elastic, it also decreases the combined temperature and shrinkage stress to some extent depending upon the relaxation coefficient.
- The results from the finite element analysis are conservative for linear static model. However, more detail study is required for analysis regarding the soil structure interaction, prestress loss in tendons, tendon geometry, etc. which may be possible with the non-linear analysis.
- The one or more supplementary measures for crack mitigation in addition to prestressing can be beneficial in reducing the construction costs. For e.g., SCC with post tensioning has been proved to be sound and cost-effective measure since post tensioning is costly when applied solely for the purpose of crack controlling of super-long structures.

ACKNOWLEDGMENT

This research is funded by the China Scholarship Council (CSC) and College of Civil Engineering, Tongji University, China.

REFERENCES

[1] "GB50010-2010, Code for design of concrete structures[S], Beijing: China Building Industry Press (English)." 2011.

[2] Z. H. -ya, "Research on Technique of Ultra-long Concrete Structure Without Joints," *Shenzhen General Institute of Architectural Design & Research, Shenzhen 518031, China*.

[3] G. Guo, L. M. Joseph, and G. E. Bieberly, "Restraint Design of Cast-in-place Post-Tensioned Underground Parking Structures.," *PTI Journal*, no. August, pp. 5–18, 2009.

[4] X. Chen, S. Wei, M. Shen, A. Zhao, and J. Cai, "No-joints design method and example for long concrete structure," *2011 International Conference on Electric Technology and Civil Engineering, ICETCE 2011 - Proceedings*. pp. 2388–2391, 2011, doi: 10.1109/ICETCE.2011.5774781.

[5] M. K. Badrah and M. N. Jadid, "Investigation of Developed Thermal Forces in Long Concrete Frame Structures," *The Open Civil Engineering Journal*, vol. 7, no. 1, pp. 210–217, 2013, doi: 10.2174/1874149501307010210.

[6] Y. Z. Yin and B. W. Li, "Study on temperature effect of the super-long concrete structure in electrolytic aluminum plants," *Applied Mechanics and Materials*, vol. 584–586, pp. 1026–1030, 2014, doi: 10.4028/www.scientific.net/AMM.584-586.1026.

[7] B. Y. P. Esselinck and D. J. Carreira, "Analysis of Shortening of Post-Tensioned Slabs," *PTI Journal*, no. December, pp. 5–18, 2016.

[8] P. Ying, K. Yejun, C. Weiwen, and X. Feng, "Analysis of temperature variation and shrinkage effects on over-long concrete

structures and engineering practice," *Building Structure*, vol. 40, no. 10, pp. 86–90, 2010.

[9] G. Espinet, "Design key technology of expansion reinforcing band for super-long concrete structures," 2017.

[10] S. A. Li Kun, "Application of Unbonded Prestressing Technology in Super-Long Structures," *Quality of Civil Engineering and Construction*, no. 8, pp. 41–43, 2004.

[11] R. Qiao, "Prestress Technology and Crack Control of Super-Long Concrete Structure," *IOP Conference Series: Earth and Environmental Science*, vol. 525, no. 1, 2020, doi: 10.1088/1755-1315/525/1/012020.

[12] L. Yong, "Analysis and Application of Unbonded Prestress in Cracks Control of Long Concrete Structure," pp. 190–191, 2000.

[13] Li Lijuan, L. Feng, G. Fu, and W. Lu, "Non-Gap Design Method and Test for Post-Tensioned Prestressed RC Structure," *Mechanics of 21st Century - ICTAM04 Proceedings*, vol. 3, no. 2, pp. 1–2, 2015.

[14] Y. Dang and Y. K. Liu, "Deformation of overlong isolated buildings caused by thermal and concrete shrinkage," *Mathematical Problems in Engineering*, 2013, doi: 10.1155/2013/139159.

[15] ACI Committee 209, "Guide for modelling and calculating shrinkage and creep in hardened concrete.," Farmington Hills, MI, 2008.

[16] N. J. Gardner, "Comparison of prediction provisions for drying shrinkage and creep of normal-strength concretes," *Canadian Journal of Civil Engineering*, vol. 31, no. 5, pp. 767–775, 2004, doi: 10.1139/L04-046.

[17] Rajeev Goel; Ram Kumar; and D. K. Paul, "Comparative Study of Various Creep and Shrinkage Prediction Models for Concrete," *Journal of Materials in Civil Engineering*, vol. 19, no. march, pp. 249–260, 2007, doi: 10.1061/(ASCE)0899-1561(2007)19.

[18] N. J. Gardner and M. J. Lockman, "Design provisions for drying shrinkage and creep of normal-strength concrete," *ACI Materials Journal*, vol. 99, no. 1, pp. 111–112, 2002.

[19] ACI Committee 209, "Prediction of Creep, Shrinkage and Temperature Effects in Concrete Structures. ACI 209R-92," Farmington Hills, MI, 2008.

[20] Concrete Society, "Post Tensioned Concrete Floors: Design Handbook (PTI TAB.1-06). Second Edition. Technical Report No. 43," Camberley, UK, 2005.

[21] PCI Committee, *PCI Design handbook—Precast and Prestressed Concrete*, Sixth Edit. Chicago, Illinois: Precast/Prestressed Concrete Institute, 2004.

[22] K. B. Bondy, "Shortening Problem in Post-Tensioned Concrete Buildings.," in *SEAOSC Seminar - Design Review and Inspection of Prestressed Concrete Building Projects*, 1989, pp. 1–19.

[23] G. Guo and L. M. Joseph., "Shortening Estimation for Post-Tensioned Concrete Floors-Part I: Model Selection.," *ACI Structural Journal*, vol. 110, no. 1, pp. 27–34, 2013.

[24] J. Sadrekarimi and M. A. Ghamari, "the Coefficient of Subgrade Reaction and Its Accuracy on Design of Foundations," *Sixth International Conference on Case Histories in Geotechnical Engineering*, pp. 1–6, 2008.

[25] D. R. Bohnhoff, "Modeling Soil Behavior with Simple Springs, Part 1," *Research & Technology*, no. April, pp. 49–54, 2014.

[26] W. Tiemeng, "Engineering structure crack control [M]. (in Chinese).," *China Building Industry Press*, pp. 211–235, 1997.

[27] P. Kohnk, *Ansys Theory Reference for the Mechanical APDL and Mechanical Applications*, no. April. Canonsburg, PA, 2009.

[28] M. Iqbal, "Thermal movements in parking structures," *ACI Structural Journal*, vol. 104, no. 5, p. 542, 2007.

[29] L. A. World, "How does shrinkage-compensating cement concrete help post-tensioning?," *Concrete Construction*, 1996.